Revista de Metalurgia
October-December 2022, 58 (4), e231
ISSN-L: 0034-8570
https://doi.org/10.3989/revmetalm.231

TiN hard coating as a candidate reference material for surface metrology in chemistry: characterization and quantification by bulk and surface analyses techniques

José Manuel Juárez-García[a*], Jorge Morales-Hernández[b], Aime Gutiérrez-Peralta[c], Edgar Cruz-Valeriano[c], Rafael Ramírez-Bon[c], José M. Yañez Limón[c]

[a]Universidad Tecnológica de Querétaro. Av. Pie de la Cuesta 2501, Nacional, 76148 Santiago de Querétaro, Qro. México

[b]Centro de Investigación y Desarrollo Tecnológico en Electroquímica S.C., Parque Tecnológico Querétaro s/n, Sanfandila, Pedro Escobedo, Querétaro, C.P. 76703, México

[c]Centro de Investigación y de Estudios Avanzados del IPN-Unidad Querétaro. Libramiento Norponiente #2000, Fraccionamiento. Real de Juriquilla, C.P. 76230, México

(*Corresponding author: jose.juarez@uteq.edu.mx)

Submitted: 18 August 2021; Accepted: 29 November 2022; Available On-line: 27 December 2022

ABSTRACT: This study presents the synthesis and characterization of TiN hard coatings as a candidate reference material for surface metrology in chemistry. TiN coatings were grown on a silicon wafer with (111) orientation using dc reactive magnetron sputtering. X-ray diffraction confirms that the diffraction phase of TiN coatings is polycrystalline, electron microscopy demonstrates that the TiN coatings presents pyramidal-shaped grains ranging from sub-micrometer to nano-size scale and with an average thickness of 666 nm. According to micro Raman results, the presence of LO phonon modes confirms that the TiN coatings are crystalline in nature and no impurities are detected. The mechanical properties at the nanoscale are evaluated using resonance tracking acoustic force atomic microscopy. The chemical composition of the TiN reveals a close 1:1 atomic ratio. The ANOVA is used to evaluate the homogeneity of the TiN via a homogeneity test according to the ISO Guide 35:2017, while, regarding the chemical composition of the Ti, the Fisher's test demonstrates that the batch can be considered as homogeneous.

KEYWORDS: ANOVA; Materials characterization; Metrology; TiN coating

Citation/Citar como: Juárez-García, J.M.; Morales-Hernández, J.; Gutiérrez-Peralta, A.; Cruz-Valeriano, E.; Ramírez-Bon, R.; Yañez Limón, J.M. (2022). "TiN hard coating as a candidate reference material for surface metrology in chemistry: characterization and quantification by bulk and surface analyses techniques". *Rev. Metal.* 58(4): e231. https://doi.org/10.3989/revmetalm.231

RESUMEN: *Recubrimientos duros de TiN como candidato a material de referencia para la metrología de superficies en química: caracterización y cuantificación mediante técnicas de análisis de superficie y de volumen*. Este estudio presenta la síntesis y caracterización de recubrimientos duros de TiN como material de referencia candidato para la metrología de superficies en química. Los recubrimientos de TiN se cultivaron en una oblea de silicio con

orientación (111) usando deposición con magnetrón reactivo dc. La difracción de rayos X confirma que los recubrimientos de TiN son policristalinos, la microscopía electrónica demuestra que los recubrimientos de TiN presentan granos de forma piramidal que van desde la escala sub-micrométrica hasta la nanométrica y con un espesor promedio de 666 nm. Según los resultados de micro-Raman, la presencia de modos de fonón LO confirma que los recubrimientos de TiN son de naturaleza cristalina y no se detectan impurezas. Las propiedades mecánicas a nanoescala se evalúan utilizando microscopía atómica de fuerza acústica de seguimiento de resonancia. La composición química del TiN revela una relación atómica cercana a 1:1. El ANOVA se utiliza para evaluar la homogeneidad del TiN mediante una prueba de homogeneidad según la Guía ISO 35:2017, mientras que, en cuanto a la composición química del Ti, la prueba de Fisher demuestra que el lote puede considerarse homogéneo.

PALABRAS CLAVE: ANOVA; Caracterización de materiales; Metrología; Recubrimiento TiN

ORCID ID: José Manuel Juárez-García (https://orcid.org/0000-0002-2303-5420); Jorge Morales-Hernández (https://orcid.org/0000-0002-8892-128X); Aime Gutiérrez-Peralta (https://orcid.org/0000-0002-4269-3357); Edgar Cruz-Valeriano (https://orcid.org/0000-0003-1787-2641); Rafael Ramírez-Bon (https://orcid.org/0000-0001-8939-6731); José M. Yañez Limón (https://orcid.org/0000-0001-6457-4044)

1. INTRODUCTION

Surface metrology and nano-metrology worldwide play a key role for measurements of advanced and emerging materials. In this way, the National Center of Metrology (CENAM, for its initials in Spanish) in Mexico has actively participated in different international groups such as the Working Group on Surface Analysis of the Comité Consultatif pour la Quantité de Matière (CCQM, for its initials in French), in the "Versailles Project on Advanced Materials and Standards" (VAMAS), and the Asia-Pacific Economic Cooperation. In a Latin-American context, the CENAM has participated in the "Mexican Society of Materials", where several research institutes as well as private and government companies are included. A substantial growth in the industrialization of technology has allowed an increasing need for researching and developing reference materials (RMs) since the existing market for these materials is still very low (Mathia *et al.*, 2011; Kim *et al.*, 2021; Wolfgang *et al.*, 2022; Ferrarini *et al.*, 2022).

As it has been largely reported in literature, hard coatings are widely used due to their tribological, morphological and structural properties as well as their chemical composition. Among these hard coatings, CNx and nitride-based compounds (TiNC, TiC and TiN), they are all broadly used due to their good hardness, they have a hardness between 15 to 40 GP, thermal conductivity between 25 to 260 W/mK and wear resistance, modulus of elasticity between 180 to 370 GP, (Caicedo *et al.*, 2006; Ipaz Caustumal and Zambrano, 2013). In this context, the titanium nitride (TiN) is a well-known compound since it is widely applied as a biocompatible material (Hussein *et al.*, 2020), protective coating (Feng *et al.*, 2017), electrodes (Mustapha and Fekkai, 2020) and diffusion barriers in microelectronics (Silva *et al.*, 2020).

It was presumed that a TiN barrier layer with a random array of pinholes could be coupled with an adaptive coating layer to limit lubricant transport to the coating surface only through those holes, thus reducing the rate of lubricant depletion in the adaptive coating layer and prolonging the life of the coating during sliding wear at elevated temperatures, Muratore *et al.* (2007).

Other applications of TiN thin films for the metal industry are, eliminates galling, fretting, micro welding, seizing and adhesive wear, smooth operation of moving components, wear resistance on precision components, holds sharp edges or corners, cavitation erosion, erosion resistance, non-stick surface, most materials will not adhere to TiN, low friction, little dimensional impact, perfect for close tolerance parts, enhances corrosion resistance, Matthews (1985). Therefore, the understanding of the thermophysical and physicochemical properties for hard coatings become important in order to manage their features as a possible candidate in what RMs are concerned.

The need for RMs –according to international normative– has allowed the synthesis of hard coating via several approaches, ISO Guide 35 (2017); ISO 20579-4 (2018). For example, chemical vapor deposition (CVD), physical vapor deposition (PVD), vacuum-arc method and magnetron-sputtering (MS) are the techniques more widely used to deposit hard coatings. Among these techniques, MS is commonly used to deposit hard transition metal nitrides and oxides, which are used in a wide range of relevant industrial coatings.

The need to compare testing results between laboratories in different countries has favored the design and synthesis to provide reference materials, known as standard samples. Since the reliability of all testing results in surface metrology and nano-metrology are completely dependent on the availability of RMs. Consequently, this work has the objective of introducing the TiN hard coating as a candidate reference material for surface metrology. Along with this, the TiN hard coating is characterized by several bulk and surface techniques. In this work, the result of interaction between the factors and the products of these factors is evaluated with the analysis of variance (ANOVA). Also, ANOVA is applied to evaluate the homogeneity of the TiN hard coating.

Currently, another problem is the lack of calibration standards that globally maintain the reliability and reproducibility of measuring results. They provide an independent reference with respect to the location, measuring device and environment. This immanently important property is a vital prerequisite to ensure a

constant and invariable quality of the producing industry and for process control. The limited number of available certified reference materials (CRMs) for thin film analysis and in parallel the growing market of novel thin film materials induces a growing gap of required calibration samples (Wolfgang *et al.*, 2022).

One example of such advanced thin films is the compound semiconductor material $Cu(In_{1-x}Ga_x)Se_2$ (shortly CIGS) which is used as an absorber material for thin film solar cells. The band gap of this CIGS material can be enhanced by increasing the Gallium (Ga) to Indium (In) ratio. Thus, by tuning the in-depth elemental distribution, the energy conversion efficiency of the device can be optimized. For such materials no certified reference materials are available to for instance use them as calibration samples for in-line process control, real-time investigations during film deposition, or quality management (Marinenko *et al.*, 2004; Ferrarini *et al.*, 2022).

2. MATERIALS AND METHODS

2.1. Materials

Initially, a magnetron-sputtering vapor deposition system (Intercovamex Sputtering V3) was optimized for the synthesis of TiN coatings, varying and optimizing the system parameters (power to use from 100 W to 500 W, working pressure 1×10^{-3} Pa to 5×10^{-3} Pa, Ti targets 98% to 99.99% of purity, nitrogen 99% purity flow from 4% to 16% mass percent in relation to the mixture of Ar/N_2, distance between target and substrate from 4 cm to 6 cm, time of deposit from 5 minutes to 12 minutes and cleaning of substrates), the temperature of the substrate was the same as that of the MS chamber, it was not possible to measure it, the equipment does not have a plate rotation.

Initially, through the MS process samples of approximately 2.5 cm^2 were obtained from the silicon wafer. These were cut to obtain a batch of 19 films of TiN on silicon (111), with an area of ~ 0.5 cm^2. The samples were labeled according to the experiment number, mounting a silicon substrate on the magnetron sputtering plate is as shown in Fig. 1, a) first, the glass object holder is placed, which is attached with the kapton tape and in the center the silicon adhered to one of its ends is placed, b) Obtaining the TiN film on the silicon substrate and on the glass object holder.

The homogeneity analysis was done by using four samples, the first and the last samples (M1 and M19) and two other samples were chosen randomly, according to the sampling theory (Rossbach and Grobecker, 1999; Chen *et al.*, 2019).

2.2. Synthesis of the coatings

The hard coatings were prepared using a DC pulsed magnetron sputtering (Intercovamex Sputtering V3) in stable regimen to sputtering titanium (target for Stanford Advance Materials, 7.5 cm diameter, 0.64 cm thick, purity >99.99 wt.-%) in N_2 (99.9%) and Ar (99.9%) mixed atmosphere. Before deposition, the chamber was pumped down to a base pressure below 3×10^{-3} Pa, and then the samples were sputter-cleared with Ar^+ ions at 800 V for 20 min. The deposition pressure was 1×10^{-5} Pa. After that, TiN hard coatings were deposited for 10 min under a mixed atmosphere, Ar + N_2. The TiN hard coatings were deposited according to the following deposition parameters: Atmosphere: Ar:N_2 (9:1); Chamber pressure: 0.4 Pa; Bias voltage: 120 V; deposition time 10 minutes; Current of titanium target: 3 A with a 381 W power; distance between target and substrate 0.05 m. A wafer of silicon with (111) orientation.

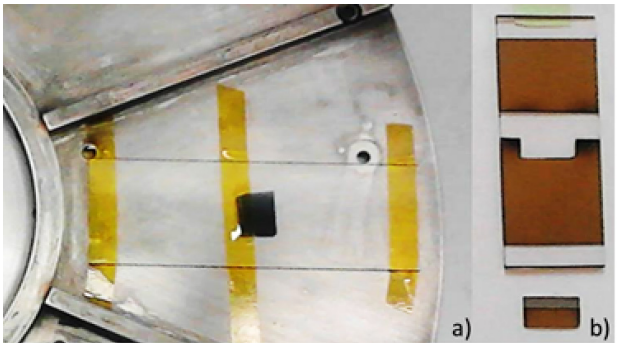

Figure 1 a) Mounting the silicon substrate on the glass object holder b) The as-deposited TiN coating on silicon substrate.

The Si (111) substrates (99.9% of purity) of 2.5 cm were obtained from a single sided polished silicon dicing wafer, 12.7 cm of diameter, 1 mm of thickness and roughness <0.5 nm, then were cleaned with phosphate-free soap and then, these were rinsed in double-distilled water. After that, the substrates were ultrasonically cleaned in an aqueous mixture (50% Xylene and 50% ethyl alcohol) for 8 minutes. Once the sonication concluded, the substrates were immersed into analytical grade ethyl alcohol. Finally, the substrates were dried under a nitrogen gas atmosphere.

2.3. Characterization of the coatings

Microstructure and chemical composition of the obtained coatings were traced by electron probe micro-analyzer (EPMA) (Rojas-Chávez *et al.*, 2018), using a JEOL JXA 8530F hyper probe, equipped with WDS and EDS detectors (Falcone *et al.*, 2006; Fazel *et al.*, 2020). The crystallographic phases were analyzed via X-ray diffraction technique (RIGAKU Dmax 2100 diffractometer), the radiation generating tube is made of Copper (Kα1=1.5406 A), The patternsX-ray diffraction were obtained with a grazing incidence angle of α= 2° and a scanning speed of 0.5°/min, step of 0.02°.

sweep angle from 30° to 80°. The structural changes of the coatings were measured using Raman spectrometry (Thermo Fisher DXR equipment), the surface of

the samples was focused with 50X objective, 50 scans were acquired for each analysis with a laser of 532 nm (green), pinhole of 50 μm, grid of 900 lines / mm (low resolution) and 9 mW of power (Spengler and Kaiser, 1976).

Resonance-Tracking Atomic Force Acoustic Microscopy (RT-AFAM) technique (Senthilkumar *et al.*, 2005; Enriquez-Flores *et al.*, 2012), was carried out on a commercial SPM system (Bruker/Veeco/Digital Instruments Nanoscope IV Dimension 3100 AFM). This AFM process was also performed with a closed-loop x–y nanopositioning stage (nPoint, Inc. NPXY100). A signal access module (SAM) accessory was used as well for interfacing the signal input/output to the AFM. The unfiltered photodiode signal input to a Stanford Research Systems SR844 high-frequency lock-in amplifier. The sweeping frequency excitation signal required was obtained by an HP/Agilent 33 120A function generator. Budget Sensors diamond-coated silicon probe, using 450 μm long with a 3.0 N/m spring constant and using a National Instruments DAQ NI-PCI-6133 card for data acquisition.

Nanoindentation, tests were done on an IBIS 2 Nanoindenter from Fischer-Cripps Laboratories, in a downward charge range of 30 mN to 12.5 mN with Vickers indenter.

The ANOVA was used to evaluate the homogeneity of the alloy via a homogeneity test according with the ISO Guide 35 (2017) and Ellison (2015), which was useful to evaluate the variability of data. Precision was estimated under repeatability conditions, whose value was obtained of 5% and –according to the results of the ANOVA– it was found that the material was homogenous (Martin and Games, 1977; Hartung *et al.*, 2002).

3. RESULTS AND DISCUSSION

3.1. X ray diffraction

The X-ray diffraction patterns in Fig. 2 indicates that the as-deposited TiN coating is highly crystalline. As it is shown in that figure, the TiN coating exhibits a NaCl-type crystal structure where five Bragg's reflections (111), (200), (220), (311) and (222) correspond to FCC-TiN. These planes were associated with the PDF file 65-0715. It is worth noting that the TiN coating shows a strong (220) preferred orientation.

The capability of the strategy used in this work is more noticeable when it is compared with other strategies used with the MS process. For example, even though Lu et al. modified the TiN preferred orientation (Lu *et al.*, 2020), they reported a poor crystallinity for the FCC-TiN when the nitrogen content was modified. Moreover, Mustapha and Fekkai reported that the substrate has a good impact on the crystalline structure of the TiN, but it affects the appearance of the Bragg's reflections (Mustapha and Fekkai, 2020).

The crystal size, from the most prominent diffraction peak, of the as-deposited TiN coating was determined using the Scherrer equation, Cullity and Stock (2001):

$$D_{hkl} = \frac{k\lambda}{\beta_{hkl}\cos\theta} \tag{1}$$

where D_{hkl} is the grain size in the direction perpendicular to the lattice planes, *hkl* are the Miller indices of the planes belonging to the diffraction peak that is being analyzed, k is the shape factor, λ = 1.54 Å is the X-ray wavelength, θ is the diffraction angle, and β_{hkl} is the full width at half maximum (FWHM) of the diffraction peak (in rad), (Cullity and Stock, 2001; Xiao *et al.*, 2007; Chen *et al.*, 2019; Silva *et al.*, 2020).

3.2. Structural and chemical analyses

TiN coatings were deposited by MS, the SEM images indicate that the as-deposited TiN film is crystalline, see Fig. 3a. Based on SEM results, in Fig. 3a, the thickness of the as-deposited TiN thin film was determined to be 0.66 ± 0.04 μm where the deviation of 0.04 μm corresponds to the calculated standard deviation, while the Ra roughness measured was 15.97 nm ± 5.5 nm. Thickness and roughness were obtained using a Bruker Contour model profilometer, GT InMotion 3D and the tool for visualization and analysis of SPM data. Based on the results of the thickness of the film, a deposit speed of 60 nm/min was obtained.

As it can be seen in Fig. 3b, the structure of the TiN coating is examined via electron microscpy, as clear-

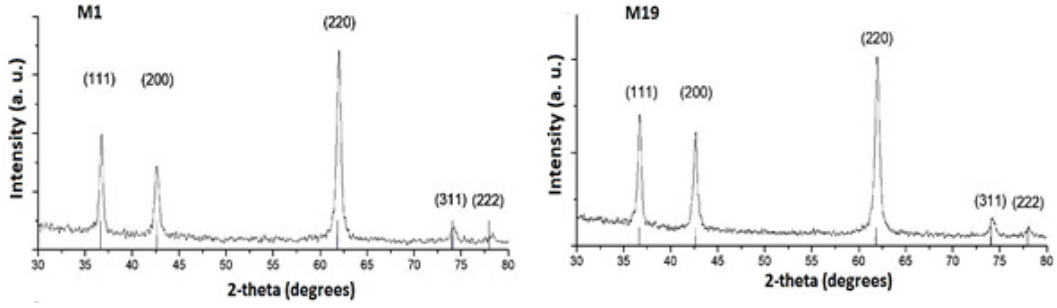

Figure 2. XRD patterns for the as-deposited TiN coating for samples M1 and M19. The Miller indices on the upper diffraction pattern correspond to the TiN compound.

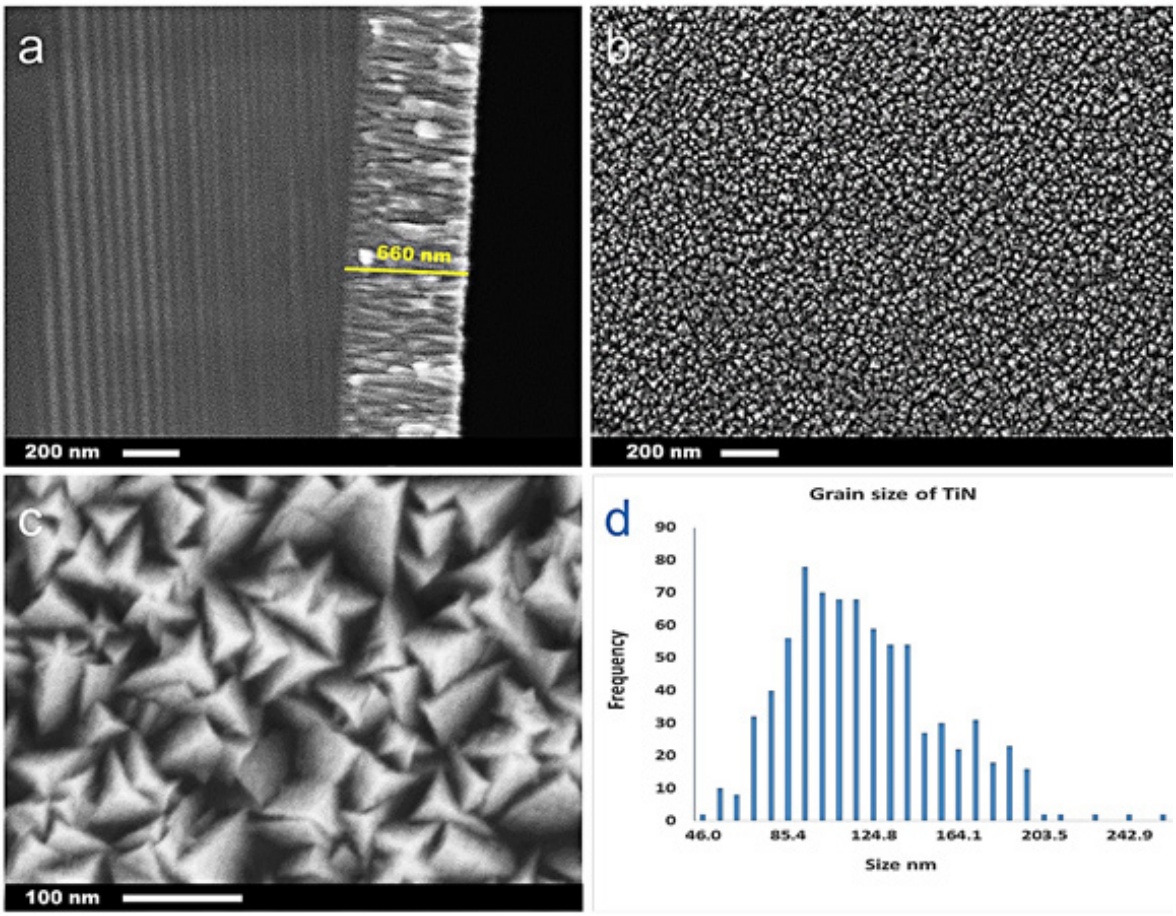

Figure 3. a) The as-deposited TiN coating with a thickness of 660 nm, magnification at 20000 X; b) SEM image of the surface of titanium nitride of sample 1, magnification at 10000 X; c) 100 000 X magnification image, randomly selected from figure b; d) Crystal size distribution of TiN by the direct measurement of the electron images, average grain size of all the samples measured, 117 ± 35.5 nm.

ly shown in this figure, the TiN presents a pyramidal-shaped grains with texture associated to the surface roughness, as it has been reported in the literature (Fazel *et al.*, 2020). That is to say, the surface of the TiN is relatively rough with a visually compact texture, see Fig. 3c. However, the morphology of TiN is ranging from the submicrometer to nano-size scale, just as it is shown in Fig. 3d. The average crystal size estimated was 117 ± 36 nm from these electron microscopy images, it was obtained by adding the two sides (1 and 2) of the crystals and then obtaining their average, Fig. 3c and 3d. Such results are in good agreement with the results obtained from Scherer's equation, crystal size found from 85 to 115 nm,

Compared with the microstructure reported by Yang *et al.* (2020), the as-deposited TiN coatings obtained in this work had the same pyramidal-shape, but without the need to vary the N_2 flow rate (Lu *et al.*, 2020; Das *et al.*, 2021).

Figure 4 shows the characteristic X-ray spectra obtained by WDS from the TiN film using the PETH, LiF and LDE2 crystals. The calibration of the crystals used for the elements of interest was done with titanium 99.99% purity and aluminum nitride 99.99% purity as references, both materials from Micro Analysis Consultants. The NIST certified reference material NIST SRM® 2061 TiAl (NbW) Alloy for Microanalysis (Marinenko *et al.*, 2004), was used as the control material, which has a certified chemical composition for Ti of 53.92 ± 0.34 mass %.

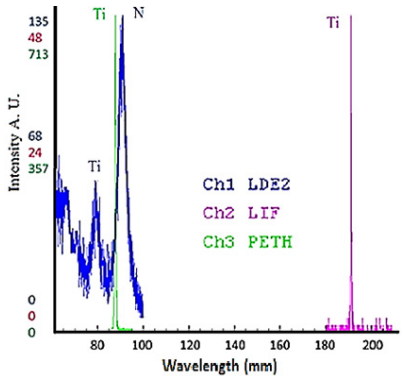

Figure 4. Characteristic X-ray wavelength spectra to determine the elemental chemical composition of Ti (LED2, PETH and LiF) and N (LDE2) in the TiN film, sample M1.

Elemental chemical composition for titanium and nitrogen was obtained from different areas on 3 different days, to evaluate repeatability and reproducibility at the surface and in the longitudinal section of the sample, to estimate the chemical composition different measurements have been carried out as highlighted in the images of Fig. 5: a) seven different areas; b) different points along the sample and c) the longitudinal section. see Fig. 5. Average chemical composition for each sample is presented in Table 1, the average was obtained from punctual and linear measurements (with a beam size of 1 µm and 20 points every 100 µm) and from the measured areas of approximately 1000 μm^2.

As shown in Table 2, the homogeneity results obtained for the thickness of the films were performed via ANOVA, the samples M1, M8, M15 and M19 were measured in triplicates.

Regarding the chemical composition of the Ti, the ANOVA and Fisher's tests demonstrated that the batch can be considered as homogeneous. Such homogeneity was supported by the analysis of variance, considering $F_{calculatgd}$=0.09 and $F_{critical}$=4.07. Therefore, the reference material candidate presented in this work meets the proper homogeneity for the intended purpose in this study.

As shown in Table 3 and Table 4, the homogeneity results obtained for the thickness of the films were performed via ANOVA, the samples M1, M8, M15 and M19 were measured in triplicates.

According to the Fisher test, the homogeneity of the batch is met when the variances among the samples are satisfied. Using the null hypothesis, it can be expressed as Ho: $F_{calculated} < F_{critical}$. For this case, it was obtained $F_{calculated}$ = 0.45 and $F_{critical}$ = 4.07 which satisfies the null hypothesis.

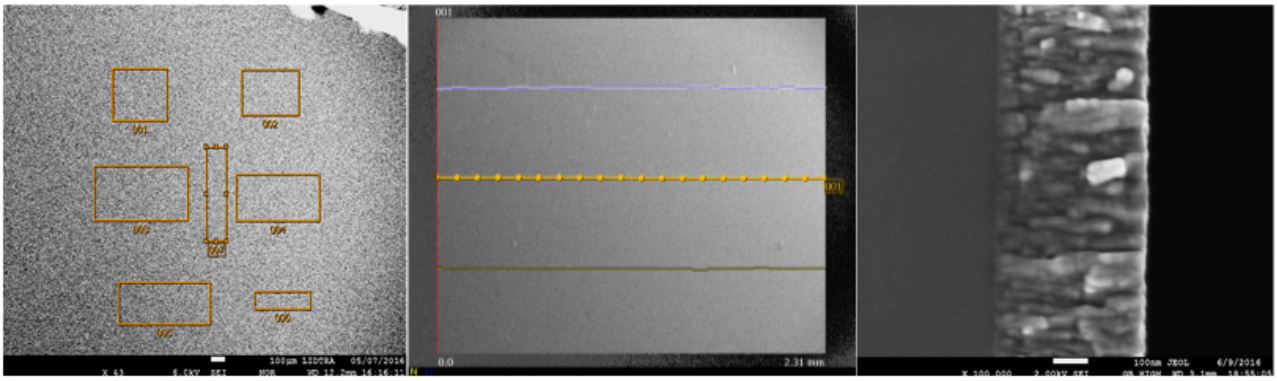

(a) (b) (c)

Figure 5. Example of the chemical analysis of Ti by EPMA: a) area, b) point and c) longitudinal section, sample.

Table 1. Results of the Ti chemical composition in the TiN films, mass-%.

Sample	Day 1	Day 2	Day 3	Average	Variance
M1	60.15	58.99	61.00	60.05	1.01
M8	59.38	58.80	61.1	59.76	1.43
M15	61.12	58.86	59.12	59.7	1.52
M19	58.16	59.23	61.2	59.53	2.37
Std. Des.	1.25	0.22	0.99	1.10	

Table 2. ANOVA to evaluate the homogeneity of the chemical composition in the TiN films.

Origin of variations	Sum of squares	Degrees of freedom	Averages of squares	F statistic	F critical value
Between groups	0.41	3	0.138	0.09	4.07
Within groups	12.71	8	1.588		
Total	13.12	11			

Table 3. Results of film thickness in nanometers.

Sample	Day 1	Day 2	Day 3	Average	Variance
M1	651	671	660	660.67	100.33
M8	655	680	661	665.33	170.33
M15	660	672	680	670.67	101.33
M19	666	650	672	662.67	129.33
Std. Des.	6.48	12.82	9.54	10.32	

Table 4. ANOVA to evaluate the homogeneity of the thickness in the TiN films.

Origin of variations	Sum of squares	Degrees of freedom	Averages of squares	F statistic	F critical value
Between groups	169	3	56.33	0.45	4.07
Within groups	1002.67	8	125.33		
Total	1171.67	11			

3.3. Micro Raman

Figure 6 shows the characteristic Raman spectra of samples M1 and M19 in the range of 100 to 900 cm^{-1}. Both spectra show strong peaks centered at 215, 328, 548 and 656 cm^{-1}. The characteristic peak at 215 cm^{-1} is assigned to transverse acoustic (TA) / longitudinal acoustic (LA) modes of TiN, while the peak at 548.71 cm^{-1} is assigned to transverse optic (TO) / longitudinal optic (LO) modes of TiN. It is worth noting that the presence of LO phonon modes confirms that the as-deposited TiN coatings are crystalline in nature (Spengler and Kaiser, 1976), which is in good agreement with the results determined by XRD and electron microscopy. Furthermore, the assigned peaks are in accordance with the reported Raman studies for TiN films (Spengler and Kaiser, 1976).

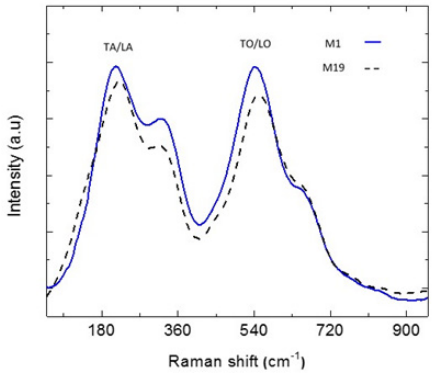

Figure 6. Raman spectra for TiN films, samples M1 and M19.

3.4. Mechanical properties

Figures 7 and 8, shows the results obtained via RT-AFAM where fused silicon was used to calibrate the equipment. In this figure, topography, frequency, elasticity modulus and the histogram of the elasticity modulus of the as-deposited TiN coating are presented. Figure 7a and Fig. 8a shows the topography of the samples M1 and M19, respectively. Although the topography shows rounded grains with size distribution larger than 50 nm, it

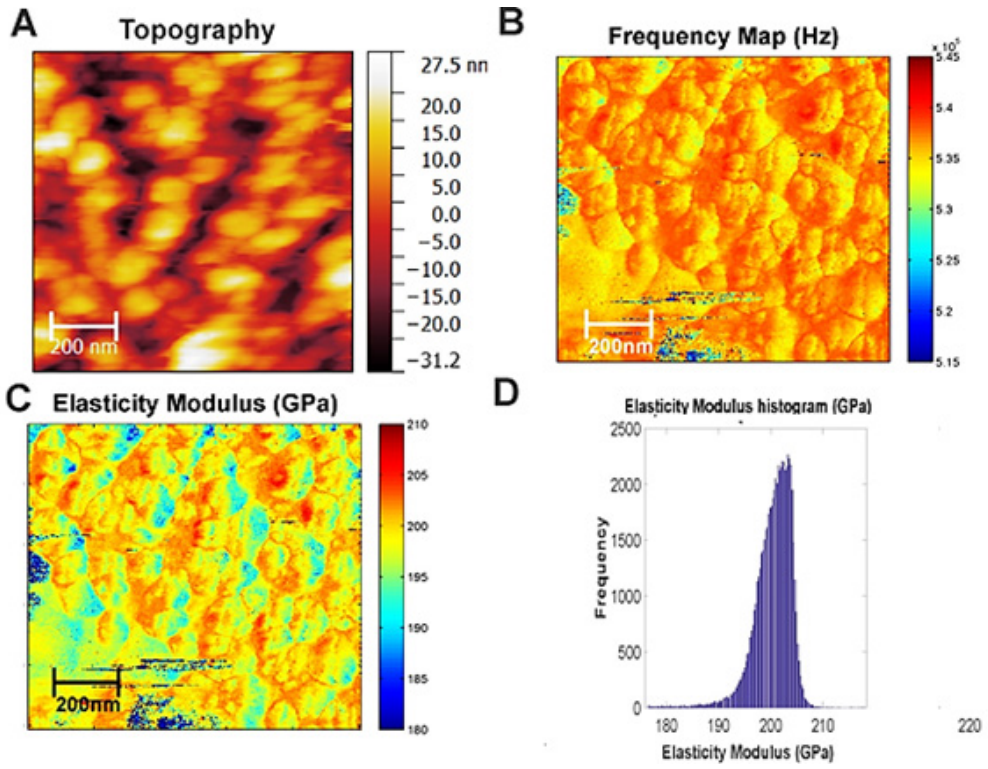

Figure 7. Data obtained from the scanning (1000 nm) of sample M1 by AFM, topography (A), frequency response from RT-AFAM (B), elasticity modulus from RT-AFAM (C), and histogram of the elasticity modulus (D).

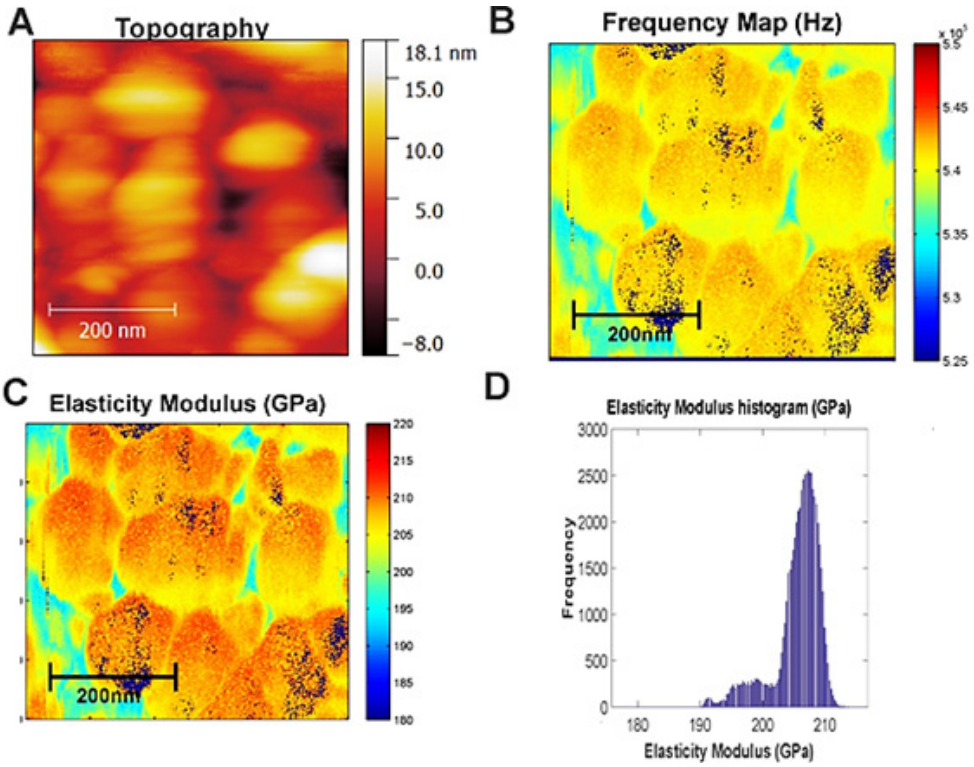

Figure 8. Data obtained from the scanning (500 nm) of sample M19 by AFM, topography (A), frequency response from RT-AFAM (B), elasticity modulus from RT-AFAM (C), and histogram of the elasticity modulus (D).

is worth keeping in mind that the XRD and the electron microscopy images showed congruent results. Additionally, it was measured a Ra roughness of ~10 nm that corresponds to a very flat surface compared with the results reported by Fazel and coworkers (Fazel *et al.*, 2020).

The frequency is shown in Fig. 7b and Fig. 8b in the range of $5.15 \times 10^5 - 5.45 \times 10^5$ Hz, the image depicts regions of common resonance frequencies as domains distributed on the surface. It is important to mention that the frequency variations detected were related to the tip–sample contact stiffness. Such changes can be associated with the topography or due to the non-uniform distribution of the elastic modulus of the sample, as has been reported in literature (Enriquez-Flores *et al.*, 2012). The resonance frequency of the widespread domains has a value of approximately 538 kHz.

In Fig. 7c and Fig. 8c, the elasticity modulus of the as-deposited TiN coating is shown. It was calculated from resonance frequency measurements, as has been reported in literature (Enriquez-Flores *et al.*, 2012). In this figure, the elastic domains are observed, the highest value of elasticity modulus is ~203 GPa, which is shown in light orange color. In the edge of this elastic domain a small area with different domain is observed, this domain has an elasticity modulus of ~195 GPa which is shown in light green color. Moreover, in the edge of these domains, a third domain is observed with ~185 GPa of elasticity modulus, which is shown in blue color. One can infer that the three domains can make a structure that benefits the hardening of the as-deposited TiN coating; that is to say, the TiN coating has the same mechanical properties. The elasticity modulus, Fig. 7c and Fig. 8c, can be more easily interpreted by means of its histogram, see Fig. 7d and Fig. 8d.

The average indentation hardness (HIT) obtained was 17 ± 3.1 GPa. Hernández *et al.* (2011) obtained comparable nanohardness values of 17.6, 31.0 to 23.3 GPa,

So far the experimental findings in the areas of chemical stability and mechanical properties show significant results to propose TiN as a reference material. Nonetheless, we suggest that further experimentation needs to be accomplished for that purpose, for example, analysis with other surface analysis techniques such as XPS for the evaluation of impurities, or analysis by wet method such as ICP-MS or ICP-MS.

4. CONCLUSIONS

- TiN coatings were grown over silicon (111) substrates using dc reactive magnetron sputtering under a mixed atmosphere, Ar+N_2. In this study the composition, microstructure and mechanical properties were investigated. The main results are shown as follows:
- The TiN coating exhibited a single FCC structure and it presented a strong (220) preferred orientation. The average grain size estimated from microscopy was in good agreement with the results obtained from Scherer's equation. In addition to

this, the presence of LO phonon modes, detected by micro Raman, confirmed that the as-deposited TiN coatings were crystalline in nature, which was in good agreement with the experimental findings determined by XRD and EPMA.

- RT-AFAM results showed that the TiN coating exhibited a nanostructure of elastic domains, being the principal elastic domain ranging from ~203 to ~208 GPa. However, the elastic domains performed like nanostructure arrangements for hardening should act as a barrier for plastic deformations, which confers a high hardness, which was similar to that reported for this type of thin films.
- Elemental chemical composition for titanium was obtained as Ti 59.7% mass fraction. The ANOVA demonstrated the homogeneity of the TiN according to the ISO Guide 35:2017, while regarding the chemical composition of the Ti, Fisher's test demonstrated that the batch can be considered as homogeneous.
- Therefore, we can state that the chemical homogeneity and microstructure properties make TiN coating an eligible material to continue with the process of certification as a reference material to evaluate the mass % of Ti in the thin films.

ACKNOWLEDGMENTS

This research was conducted as a part of a materials certification process of CENAM, within the research activities of LIDTRA through the project LN2015-254119 of CONACYT Mexico and also through the TecNM program, support for scientific and technological research 2017 -project 616117-P. Authors are gratefully acknowledge the SNI for the distinction of their membership.

REFERENCES

Caicedo, J.C., Gómez de Prieto, M.E. (2006). Producción y Caracterización de Superredes de Nitruro de Titanio-Nitruro de Zirconio como Recubrimientos duros sobre Acero para Sustitución de un producto Importado en el Corte del Papel. Tesis de Pregrado, Universidad del Valle, Santiago de Cali, Colombia.

Cullity, B.C., Stock, S.R. (2001). *Elements of X-Ray Diffraction*. 3rd Ed., Prentice-Hall Inc., pp. 96-102.

Chen, S.X., Li, J., Zhong, P.S. (2019). Two-sample and ANOVA tests for high dimensional means. *Ann. Stat.* 47 (3), 1443–1474. https://doi.org/10.1214/18-AOS1720.

Das, S., Guha, S., Ghadai, R., Swain, B.P. (2021). A comparative analysis over different properties of TiN, TiAlN and TiAlSiN thin film coatings grown in nitrogen gas atmosphere. *Mater. Chem. Phys.* 258, 123866. https://doi.org/10.1016/j.matchemphys.2020.123866.

Ellison, S.L.R. (2015). Homogeneity studies and ISO Guide 35:2006. *Accred. Qual. Assur.* 20, 519–528. https://doi.org/10.1007/s00769-015-1162-z.

Enriquez-Flores, C.I., Gervacio-Arciniega, J.J., Cruz-Valeriano, E., De Urquijo-Ventura, P., Gutierrez-Salazar, B.J., Espinoza-Beltran, F.J. (2012). Fast frequency sweeping in resonance-tracking SPM for high-resolution AFAM and PFM imaging. *Nanotechnology* 23, 495705. https://doi.org/10.1088/0957-4484/23/49/495705.

Falcone, R., Sommariva, G., Verità, M. (2006). WDXRF, EPMA and SEM/EDX quantitative chemical analyses of small glass samples. *Mikrochim. Acta* 155, 137–140. https://doi.org/10.1007/s00604-006-0531-z.

Fazel, Z.A., Elmkhah, H., Fattah-Alhosseini, A., Babaei, K., Meghdari, M. (2020). Comparing electrochemical behavior of applied CrN/TiN nanoscale multilayer and TiN single-layer coatings deposited by CAE-PVD method. *J. Asian Ceram. Soc.* 8, 510–518. https://doi.org/10.1080/21870764.2020.1756065.

Feng, X., Zhang, Y., Hu, H., Zheng, Y., Zhang, K., Zhou, H. (2017). Comparison of mechanical behavior of TiN, TiNC, CrN/TiNC, TiN/TiNC films on 9Cr18 steel by PVD. *Appl. Surf. Sci.* 422, 266–272. https://doi.org/10.1016/j.apsusc.2017.05.042.

Ferrarini, P., Lamagna, L., Revello, F.D. (2022). *Thin Films Characterization and Metrology. In: Silicon Sensors and Actuators*. Vigna, B., Ferrari, P., Villa, F.F., Lasalandra, E., Zerbini, S. (Eds), Springer. https://doi.org/10.1007/978-3-030-80135-9_4.

Hartung, J., Argaç, D., Makambi, K.H. (2002). Small sample properties of tests on homogeneity in one-way Anova and meta-analysis. *Stat. Pap.* 43, 197–235. https://doi.org/10.1007/s00362-002-0097-8.

Hernández, L.C., Ponce, L., Fundora, A., López, E., Pérez, E. (2001). Nanohardness and Residual Stress in TiN Coatings. *Materials* 4 (5), 929-940. https://doi.org/10.3390/ma4050929.

Hussein, M.A., Adesina, A.Y., Kumar, A.M., Sorour, A.A., Ankah, N., Al-Aqeeli, N. (2020). Mechanical, in-vitro corrosion, and tribological characteristics of TiN coating produced by cathodic arc physical vapor deposition on Ti20Nb13Zr alloy for biomedical applications. *Thin Solid Films* 709, 138183. https://doi.org/10.1016/j.tsf.2020.138183.

Ipaz Cuastumal, L.M., Zambrano, G.A. (2013). Propiedades Mecánicas y Tribológicas de Recubrimientos Ternarios Nanoestructurados basados en Titani, Aluninio y Cromo obtenidos por el Método de Co-Sputtering. Tesis doctoral, Universidad del Valle, Santiago de Cali, Colombia.

ISO Guide 35 (2017). Reference materials - Guidance for characterization and assessment of homogeneity and stability.

ISO 20579-4 (2018). Surface chemical analysis - Guidelines to sample handling, preparation and mounting - Part 4: Reporting information related to the history, preparation, handling and mounting of nano-objects prior to surface analysis.

Kim, K.J., Kim, A., Kim, C.S., Song, S.W., Ruh, H., Unger, W.E.S., Radnik, J., Mata-Salazar, J., Juarez-García, J.M., Cortazar-Martínez, O. (2021), Thickness measurement of nm HfO_2 films. *Metrologia* 58, 1A. https://doi.org/10.1088/0026-1394/58/1A/08016.

Lu, G., Yu, L., Ju, H., Zuo, B., Xu, J. (2020). Influence of nitrogen content on the thermal diffusivity of TiN films prepared by magnetron sputtering. *Surf. Eng.* 36 (2), 192–198. https://doi.org/10.1080/02670844.2019.1646964.

Marinenko, R.B., Sieber, J.R., Yu, L.L., Butler, T.A., Leigh, S. (2004). A New NIST SRM® for Microanalysis and X-ray Fluorescence, TiAl(NbW) Alloy. *Microsc. Microanal.* 10 (2), 926-927. https://doi.org/10.1017/S1431927604884708.

Martin, C.G., Games, P.A. (1977). Anova Tests for Homogeneity of Variance: Nonnormality and Unequal Samples. *J. Educ. Stat.* 2 (3), 187–206. https://doi.org/10.3102/10769986002003187.

Mathia, T.G., Pawlus, P., Wieczorowski, M. (2011). Recent trends in surface metrology. *Wear* 271 (3-4), 494–508. https://doi.org/10.1016/j.wear.2010.06.001.

Matthews, A. (1985). Titanium Nitride PVD Coating Technology. *Surf. Eng.* 1(2), 93-104, https://doi.org/10.1179/sur.1985.1.2.93.

Muratore, C., Hu, J.J., Voevedin, A.A. (2007). Adaptive nanocomposite coatings with a titanium nitride diffusion barrier mask for high-temperature tribological applications. *Thin Solid Films* 515 (7–8). https://doi.org/10.1016/j.tsf.2006.09.051.

Mustapha, N., Fekkai, Z. (2020). Impact of nitrogen reactive gas and substrate temperature on the optical, electrical and structural properties of sputtered TiN thin films. *J.*

Mater. Sci. Mater. Electron. 31, 20009–20021. https://doi.org/10.1007/s10854-020-04523-z.

Rojas-Chávez, H., González-Domínguez, J.L., Román-Doval, R., Juárez-García, J.M., Daneu, N., Farías, R. (2018). ZnTe semiconductor nanoparticles: A chemical approach of the mechanochemical synthesis. *Mater. Sci. Semicond. Process.* 86, 128–138. https://doi.org/10.1016/j.mssp.2018.06.029.

Rossbach, M., Grobecker, K.-H. (1999). Homogeneity studies of reference materials by solid sampling - AAS and INAA. *Accred. Qual. Assur.* 4, 498–503. https://doi.org/10.1007/s007690050422.

Senthilkumar, V., Venkatachalam, S., Viswanathan, C., Gopal, S., Narayandass, S.K., Mangalaraj, D., Wilson, K.C., Vijayakumar, K.P. (2005). Influence of substrate temperature on the properties of vacuum evaporated InSb films. *Cryst. Res. Technol.* 40 (6), 573–578. https://doi.org/10.1002/crat.200410385.

Silva, F.C., Tunes, M.A., Sagás, J.C., Fontana, L.C., De Lima, N. B., Schön, C.G. (2020). Mechanical properties of homogeneous and nitrogen graded TiN thin films. *Thin Solid Films* 710, 138268. https://doi.org/10.1016/j.tsf.2020.138268.

Spengler, W., Kaiser, R. (1976). First and second order Raman scattering in transition metal compounds. *Solid State Commun.* 18 (7), 881–884. https://doi.org/10.1016/0038-1098(76)90228-3.

Wolfgang, E.S., Unger, Fujimoto, T. (2022). The Surface Analysis Working Group at the Consultative Committee for Amount of Substance, Metrology in Chemistry and Biology: A successful initiative by Martin Seah. *Surf. Interface Anal.* 54 (4), 314-319. https://doi.org/10.1002/sia.7033.

Xiao, L., Yan, D., He, J., Zhu, L., Dong, Y., Zhang, J., Li, X. (2007). Nanostructured TiN coating prepared by reactive plasma spraying in atmosphere. *Appl. Surf. Sci.* 253 (18), 7535–7539. https://doi.org/10.1016/j.apsusc.2007.03.062.

Yang, Y., Wang, T., Yao, T., Li, G., Sun, Y., Cao, X., Ma, L., Peng, S. (2020). Preparation of a novel TiN/TiNxOy/SiO_2 composite ceramic films on aluminum substrate as a solar selective absorber by magnetron sputtering. *J. Alloys Compd.* 815, 152209. https://doi.org/10.1016/j.jallcom.2019.152209.